Turkish Journal of Electrical Engineering & Computer Sciences

http://journals.tubitak.gov.tr/elektrik/

Research Article

Turk J Elec Eng & Comp Sci
(2019) 27: 499 – 515

doi:10.3906/elk-1804-147

Detection of hemorrhage in retinal images using linear classifiers and iterative thresholding approaches based on firefly and particle swarm optimization algorithms

Kemal ADEM[1*], **Mahmut HEKİM**[2], **Selim DEMİR**[3]

[1]Department of Informatics, Faculty of Arts and Sciences, Tokat Gaziosmanpaşa University, Tokat, Turkey
[2]Department of Electrical and Electronics Engineering, Faculty of Engineering, Tokat Gaziosmanpaşa University, Tokat, Turkey
[3]Department of Ophthalmology, Faculty of Medicine, Tokat Gaziosmanpaşa University, Tokat, Turkey

Received: 20.04.2018 • **Accepted/Published Online:** 26.06.2018 • **Final Version:** 22.01.2019

Abstract: We propose a novel iterative thresholding approach based on firefly and particle swarm optimization to be used for the detection of hemorrhages, one of the signs of diabetic retinopathy disease. This approach consists of the enhancement of the image using basic preprocessing methods, the segmentation of vessels with the help of Gabor and Top-hat transformation for the removal of the vessels from the image, the determination of the number of regions with hemorrhages and pixel counts in these regions using firefly algorithm (FFA) and particle swarm optimization algorithm (PSOA)-based iterative thresholding, and the detection of hemorrhages with the help of a support vector machine (SVM) and linear regression (LR)-based classifier. In the preprocessing step, color space selection, brightness and contrast adjustment, and adaptive histogram equalization are applied to enhance retinal images, respectively. In the step of segmentation, blood vessels are detected by using Gabor and Top-hat transformations and are removed from the image to avoid confusion with hemorrhagic regions in the retinal image. In the iterative thresholding step, the number of hemorrhagic regions and pixel counts in these regions are determined by using an iterative thresholding approach that generates different thresholding values with the FFA/PSOA. In the classification step, the hemorrhagic regions and pixel counts obtained by the iterative thresholding are used as inputs in the LR/SVM-based classifier. PSOA-based iterative thresholding and the SVM classifier achieved 96.7% sensitivity, 91.4% specificity, and 94.1% accuracy for hemorrhage detection. Finally, the experiments show that the correct classification rates and time performances of the PSOA-based iterative thresholding algorithm are better than those of the FFA in hemorrhage detection. In addition, the proposed approach can be used as a diagnostic decision support system for detecting hemorrhages with high success rate.

Key words: Hemorrhage, firefly algorithm, particle swarm optimization algorithm, iterative thresholding

1. Introduction

Diabetes-induced diabetic retinopathy (DR) is the leading cause of blindness and reduction in visual acuity worldwide [1]. It is estimated that around 93 million people in the world have DR and therefore about 28 million people suffer from this loss of vision [2]. Although there are many factors effective in DR, the most significant factor is the advanced glycation end-products caused by increased blood glucose. This deterioration of the blood vessel walls leads to bubbles, obstructions, and leaks in the blood vessels, as well. Diabetes-induced microvascular and macrovascular complications are seen in the retinal blood vessels as well as all blood

*Correspondence: kemal.adem@gop.edu.tr

vessels in the body. Coronary artery occlusion and stroke due to the obstruction of cerebral vessels are the major systemic vascular events that pose a life-threatening risk because of diabetes [3]. It is very important to monitor these diseases periodically without the need for surgical intervention for retinal vascular circulation. In this regard, the datasets obtained by retinal examination are indicative of systemic involvement of diabetes. Comprehensive study results in the United States show that 34% to 89% of people with DR are at risk of death [4]. Hemorrhage is bleeding in vessels caused by the damage occurring in the blood barrier due to the rupture of the capillaries and the microaneurysms present in the retina, which is the most basic characteristic symptom of DR. In addition, other symptoms of DR are soft exudate, hard exudate, and neovascularization [5].

The studies related to the automatic detection of hemorrhages can be classified into 5 groups as matched filter, morphological operations, Gabor transformation, statistical features, and other image processing techniques. In the studies based on matched filters, the success rates were 82.4% on 84 images [6], 84% on 68 images [7], 56% on 20 images [8], 100% on 89 images [9], and 95.04% on 20 images [10], where the filters follow the preprocessing steps of color space transformation and adaptive histogram equalization on the retinal images. In some of the studies based on basic morphological operations such as opening, closing, dilation, and erosion, the success rates were 84.1% on 30 images [11] and 84.49% on 15 images [12], and in some of the studies based on the Top-hat transformation, the success rates were 88.5% on 94 images [13] and 99.12% on 20 images [14]. In another study based on the Bottom-hat transformation, bringing the edges of the retinal images into the forefront, the success rate was 92.19% on 89 images [15]. In the Gabor transformation-based studies, the success rates were 90.24% on 120 images [16], 93.71% on 20 images [17], 93.1% on 20 images [18], 99.4% on 130 images [19], 98.12% on 1410 images [20], and 94.76% on 89 images [21], with the help of image processing methods such as color space transformation, adaptive histogram equalization, Gabor wavelet transformation, etc., respectively. In the studies based on statistical features, the success rates were 97.99% on 80 images [22], 73.8% on 301 images [23], 96.7% on 89 images [24], 97.2% on 1200 images [25], 89.23% on 50 images [26], 89% on 89 images [27], and 86% on 243 images [28] with the analysis of statistical features of images such as means, standard deviation, variance, contrast, and skewness after applying the color space transformations, contrast and brightness adjustment, and adaptive histogram equalization preprocessing to the retinal images. In the studies based on HSV color space transformation and the Gauss filter, the success rates were 86.62% on 60 images [29] and 92% on 143 images [30].

In this study, two different iterative thresholding approaches based on the firefly (FFA) and particle swarm optimization (PSOA) algorithms are proposed for detecting hemorrhages, which are one of the symptoms of diabetic retinopathy disease. For this purpose, retinal images obtained by a medical imaging system are enhanced by applying color space selection, brightness-contrast adjustment, and adaptive histogram equalization preoperations. Blood vessels are detected by using Gabor and Top-hat transformations to avoid confusion with areas containing hemorrhages in the retinal image, respectively. The number of pixels containing hemorrhage and the number of hemorrhagic regions are determined by using an iterative thresholding approach based on the FFA or PSOA. Hemorrhages in retinal images are detected by using these two feature datasets as inputs for the support vector machine (SVM) and linear regression (LR)-based classifier. The results of experiments implemented to compare the correct classification ratios and the time performances of the FFA and PSOA show that the PSOA-based thresholding approach reaches higher success rates in the detection of hemorrhages in retinal images.

2. Materials and methods

2.1. Dataset

The retinal images used in this study were obtained from patients admitted to the Gaziosmanpaşa University Faculty of Medicine's Department of Ophthalmology. Of the 100 images taken, 50 samples were from DR patients with hemorrhage, and another 50 were from DR patients without hemorrhage. The color images taken by digital fundus camera at a 50 degree viewing angle were in 3008×1960 resolution, 24-bit jpg image format. In the experiments, MATLAB R2017a software was used on an i7-4700 model computer with 4 GB memory.

2.2. Hemorrhage detection using optimization-based iterative thresholding approach

Thresholding is one of the simplest and popular techniques to perform segmentation based on only the brightness value of the image. Thresholding is faster than methods performing segmentation using multiple features of the image. However, although thresholding is preferred in real-time segmentation applications, it does not give a good segmentation result for each image [31]. In this study, the algorithm steps offered to overcome this problem by producing different threshold values for each retinal image, which includes the FFA-based iterative thresholding approach and the LR-based classifier, are as follows:

Step 1: To apply preprocessing methods to the retina image, first select the color space, then enhance the brightness contrast and finally equalize the adaptive histogram.

Step 2: Apply Gabor transformation and Top-hat transformation for detecting blood vessels, and then remove them from the retinal image.

Step 3: Convert the retinal images without blood vessels into a binary image using the offered iterative thresholding algorithm based on the FFA.

Step 4: Determine the number of regions and pixel counts containing hemorrhages in the binary image.

Step 5: Apply the number of regions and pixel counts to the input of the LR-based classifier to detect the hemorrhages in images.

In this paper, the most successful solution from the 4 different varieties, which are FFA/PSOA-based iterative thresholding approaches and LR/SVM-based classifier, was selected as the optimum algorithm.

2.2.1. Preprocessing

In the preprocessing step, RGB, HSV, and YIQ color spaces were applied to the retina images. Experimental studies showed that vessels and hemorrhages were more prominent when the green channel of the RGB color space were used. The retinal image was moved to the green channel of the RGB color space to bring the blood vessels and hemorrhaged regions in the image into the forefront. Figure 1 shows a raw retinal image and the retinal image obtained by color space transformation on the green channel of RGB.

In the second step, an adaptive histogram equalization method was applied to improve the brightness and contrast of the green channel image. In general, a histogram trapped in a narrow area shows a lack of contrast. To improve the image, the brightness of each pixel is transformed into a new brightness value to convert the image histogram into a desired form. If the image histogram does not cover all the brightness levels, the minimum and maximum color values are adjusted to cover all brightness levels, for performing contrast enhancement [32]. In the adaptive histogram equalization method, the image is divided into rectangular regions

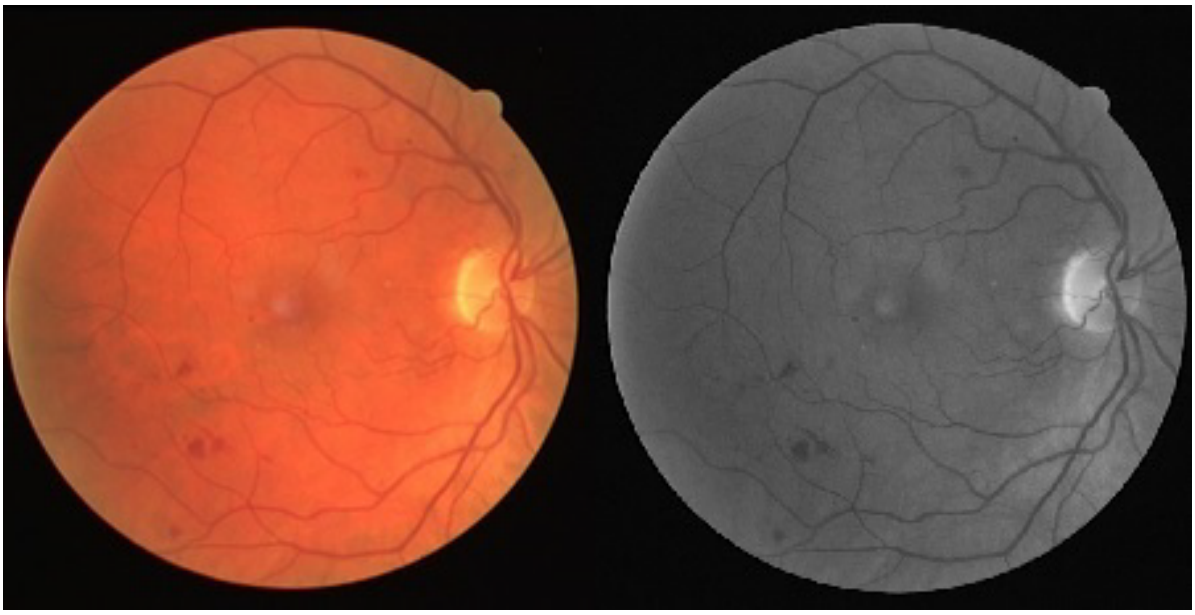

Figure 1. Retinal image and green channel of RGB color space.

and standard histogram equalization is applied to each region. After the histogram equalization process is applied to the subregions, they are combined through bilinear interpolation method to obtain an enhanced image [33]. Figure 2 shows the green channel image, its histogram, the enhanced image obtained by applying the adaptive histogram equalization, and the resulting histogram.

As shown in Figure 2, the vessels and hemorrhagic regions became more apparent thanks to the normalized histogram obtained by preprocessing of the retinal image.

2.2.2. Segmentation and removal of blood vessels from the image

The processes used to distinguish retinal vessels from the hemorrhagic regions of similar structure to avoid confusion are as follows:

2.2.2.1. Gabor transformation

Gabor transformation is an image processing algorithm used for the detection of features and edges extending in certain directions in the image. Since this conversion method is a direction-based filter due to its overall nature, it is frequently used in plate recognition processes, character recognition, and facial recognition [34]. The steps of this algorithm can be summarized as follows:

Step 1: Convert the image into a two-dimensional matrix in the form of $I(x,y)$.

Step 2: Assign the most appropriate values by testing the values of the parameters $(\tau,\theta,\sigma,\gamma)$ required for the Gabor transformation. Here, τ is the wavelength of the corresponding pattern, θ is the angle of the corresponding pattern, σ is the scale of the corresponding pattern, and γ is the aspect ratio of the Gabor core. In this study, the most appropriate values of τ, θ, σ, and γ parameters are determined as 4, 30, 1, and 0.5, respectively.

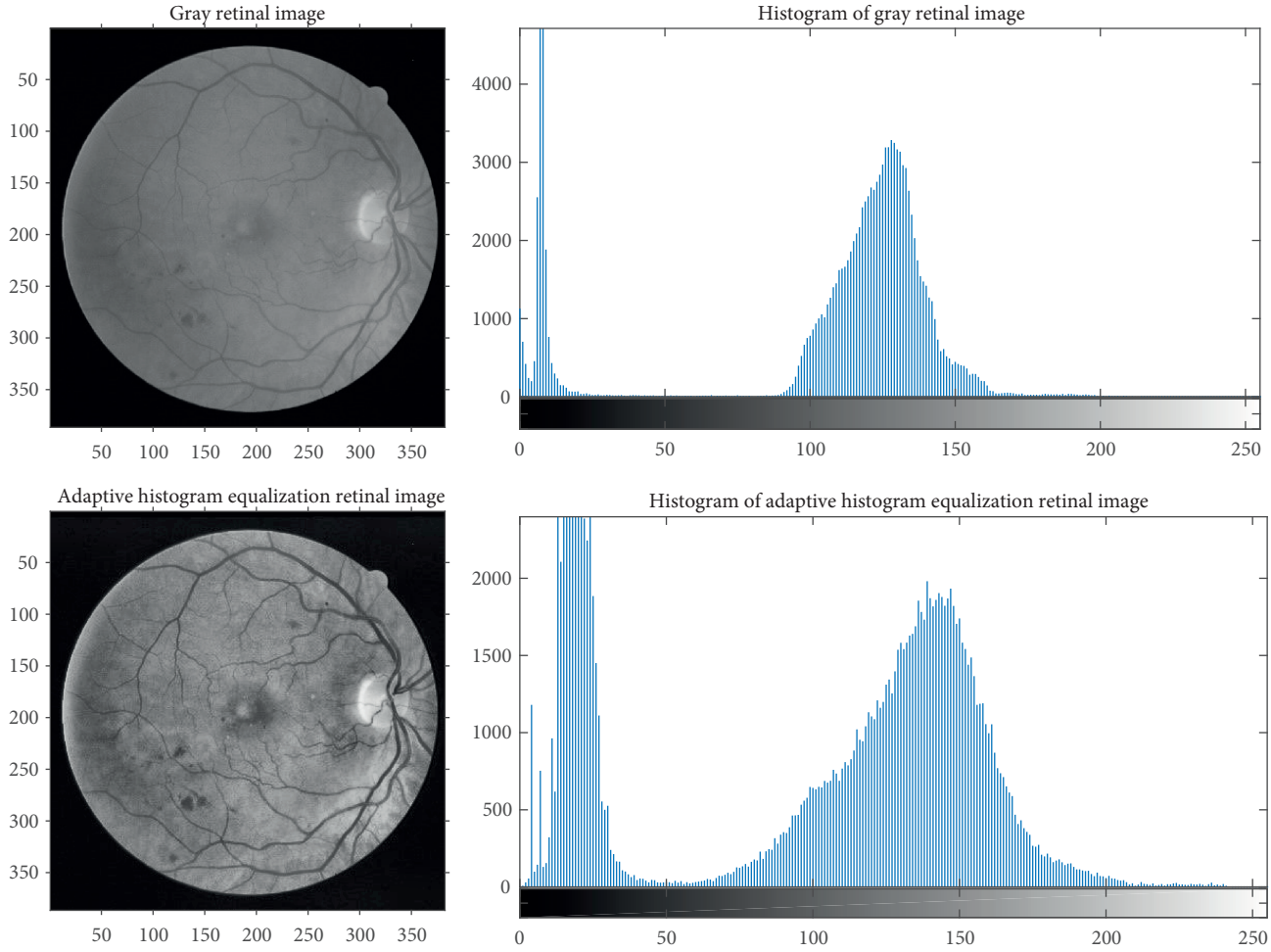

Figure 2. Image and histogram obtained with brightness-contrast adjustment and adaptive histogram equalization.

Step 3: Calculate the required $(x^{'}, y^{'})$ values in Gabor transformation using Eq. (1).

$$\begin{aligned} x^{'} &= x\cos\theta + y\sin\theta \\ y^{'} &= y\cos\theta - x\sin\theta \end{aligned} \tag{1}$$

Step 4: Calculate the wavelet core used in Gabor transformation with Eq. (2).

$$g(x, y, \tau, \theta, \sigma, \gamma) = \exp(-\frac{(x^{'})^2 + \gamma^2(y^{'})^2}{2\sigma^2})\cos(2\pi\frac{x^{'}}{\tau}) \tag{2}$$

Step 5: Apply the resulting Gabor filter to the image (convolution of the Gabor core with the image).

Six different Gabor cores obtained by rotating the Gabor core at intervals of 30 were used to obtain six different images through convolution with the image enhanced in the previous step. From these images, the image with higher average brightness was considered the output image. Figure 3 shows the retinal image obtained by Gabor transformation.

As shown in Figure 3, the Gabor transformation allows the vessels to be more distinct and nonvascular regions to remain in the background.

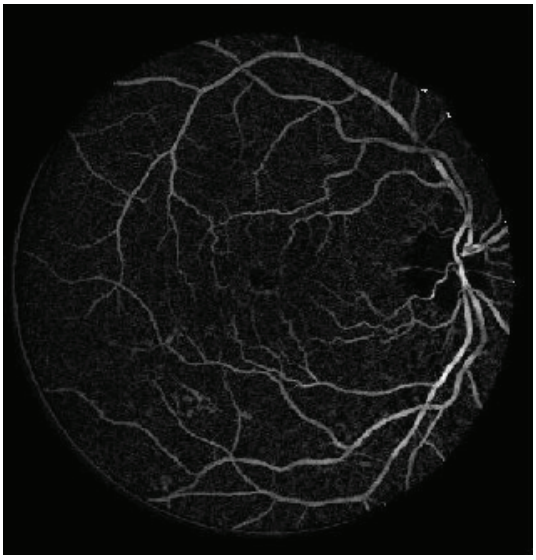

Figure 3. Retinal image obtained by Gabor transformation.

2.2.2.2. Top-hat transformation

The Top-hat transformation is a method that increases the contrast between the levels of brightness in an image and reveals the bright spots in the image; in other words, it is a method that reveals the dip and peak regions in the image. It is obtained by removing the morphologically opened image from the original image [35]. The general expression of the Top-hat transformation is as shown in Eq. (3) below.

$$top(x) = x - (x \circ (nxY)) \tag{3}$$

In Eq. (3), x refers to the image, Y is the structural factor, and n is the scale factor of the Top-hat transformation. Figure 4 shows the image obtained after applying the Top-hat transformation.

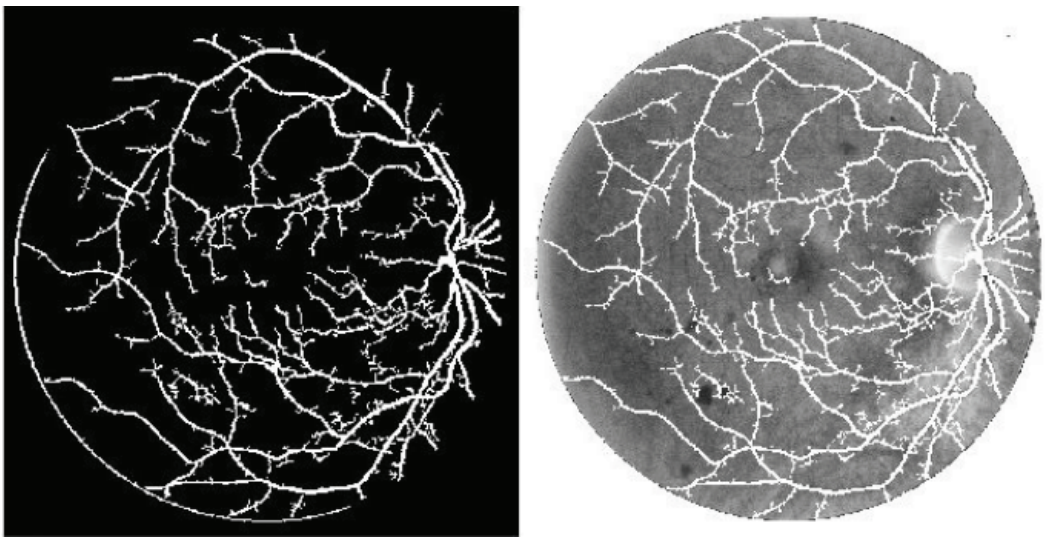

Figure 4. Application of the Top-hat transformation and removal of blood vessels from the image.

As shown in Figure 4, vessels were brought into to the forefront by the application of the Top-hat transformation to the Gabor-transformed retinal image. The vascular map obtained by Top-hat transformation is superimposed on the previously created green channel retinal image to facilitate the detection of areas containing hemorrhages.

2.2.3. Iterative thresholding based on FFA and PSOA

The approaches that produce different threshold values for each image to detect hemorrhages after segmentation and removal of blood vessels from retinal images are as follows:

2.2.3.1. Iterative thresholding based on firefly algorithm

The FFA is a swarm-based algorithm that simulates the brightness behaviors of fireflies in nature [36]. In this study, the FFA iterative thresholding algorithm was applied based on the following 3 rules for the detection of hemorrhages, which are significant symptoms of DR.

1. The gender difference is not important for all fireflies, and they can affect each other regardless of gender.
2. The effectiveness of fireflies depends on their brightness rate. Fireflies with low brightness will move towards higher ones. If there is no brighter firefly, it will move randomly.
3. The brightness of fireflies is determined by the objective function used in the problem.

There are two problems with the firefly algorithm, such as the difference in brightness intensity and the formulation of the effectiveness ratio. The effectiveness of a firefly is determined by the brightness value calculated depending on the objective function. The value of I, which indicates the brightness intensity of a firefly, is calculated by Eq. (4):

$$I = I_0 e^{-\gamma r} \tag{4}$$

The I_0 value given in Eq. (4) shows the initial brightness intensity, γ is the constant brightness absorption coefficient, and r is the distance between two fireflies. The effectiveness of fireflies depends on two factors, namely the brightness and distance, and the effectiveness value β is calculated by Eq. (5):

$$\beta = \beta_0 e^{-\gamma r^2} \tag{5}$$

The β_0 value given in Eq. (5) is in the range of 0–1 and shows the effectiveness when the distance between two fireflies is 0. The distance between two different fireflies of i and j is calculated using Eq. (6).

$$r_{ij} = \sqrt{(x_i - x_j)^2 + (y_i - y_j)^2} \tag{6}$$

Eq. (6) shows the calculation of the distance between two different fireflies. Here, the movement of firefly i towards firefly j, which has stronger effectiveness, is calculated by Eq. (7):

$$x_i^{t+1} = x_i + \beta_0 e^{(-\gamma r_{ij}^2)}(x_j - x_i) + \alpha(r - \frac{1}{2}) \tag{7}$$

The second term in Eq. (7) shows the rate of effectiveness, whereas the third term includes parameters such as α and r that can have random values between [0–1] with homogeneous distribution. In practice, the α, β_0, and

Table 1. The parameter values of FFA used in the study.

Parameter	Value
Number of iterations (t)	50
Number of fireflies (K)	500
Absorption coefficient (γ)	0.05
Effectiveness value for r = 0 (β_0)	0.95
Step size control (α)	0.5

γ values are chosen in the range of [0,1]. These values depend on the application results, and the parameters determined experimentally are shown in Table 1.

The iterative thresholding algorithm based on the firefly algorithm with the parameter values given in Table 1 consists of the following steps:

Step 1: Update the initial parameters of the firefly algorithm according to the values given in Table 1.

Step 2: Calculate the brightness, effectiveness values, and distances between the randomly placed fireflies in the green channel retinal image with removed vessels, according to Eqs. (4), (5), and (6).

Step 3: Compare the effectiveness values of fireflies according to the objective function given in Eq. (8). Use Eq. (7) to update the position of fireflies towards the more effective ones.

$$f(x) = \sum_{i=1}^{n} c(x) \tag{8}$$

Here, $f(x)$ is the objective function, n is the number of fireflies, and $c(x)$ is the value of the brightness of the pixel.

Step 4: Did the number of iterations end?

Step 5: Go to Step 2 if the number of iterations did not end.

Step 6: If the iterations ended, calculate the average of the brightness values at the end positions of the fireflies and select this new value as the iteration threshold value.

According to the steps of this algorithm, the first 500 fireflies are distributed on random pixels in the image, and these pixel values are assumed as the brightness value of the fireflies. In the proposed algorithm, the movement of fireflies is carried out towards the fireflies with low brightness by comparing the fireflies in terms of brightness according to Eq. (7). This process is repeated 50 times, and the brightness average of the positions of the fireflies is determined as the threshold value. Figure 5 illustrates the images obtained with the FFA. As shown in Figure 5, an iterative threshold value is generated with the FFA in order to detect areas containing hemorrhage in the retina. In this way, a different threshold value is created in each image.

2.2.3.2. Iterative thresholding based on particle swarm optimization algorithm

The PSOA is a swarm-based algorithm that simulates the movements of birds and fish moving in swarms in nature as proposed by Eberhart and Kennedy in 1995. The PSOA is based on sharing information regarding the

Figure 5. a) Distribution of fireflies in the image, b) hemorrhage detection by thresholding, c) areas containing hemorrhage in the retina.

social behaviors among individuals. Everyone is called a particle, and a collection of particles is called a swarm. Each particle position is adjusted to the best position by taking advantage of previous position experiences. This process is repeated until reaching a termination criterion, such as number of iterations [37]. The steps of the iterative thresholding algorithm with the PSOA are listed as follows:

Step 1: Create the initial swarm by assigning initial positions and velocities to the particles generated randomly on the green channel retinal image with removed vessels.

Step 2: Calculate the fitness values of all the particles in the swarm according to the objective function.

Step 3: Find the local best ($pbest$) for each particle in the current iteration. The number of the bests in the swarm corresponds to the number of particles.

Step 4: Select the global best ($gbest$) from local bests in the current iteration.

Step 5: Update the position and velocity of the particles according to Eqs. (9) and (10) below.

$$v_i^{k+1} = v_i^k + c_1^k(rand_1)(pbest_i^k - x_i^k) + c_2^k(rand_2)(gbest_i^k - x_i^k) \tag{9}$$

$$x_i^{k+1} = x_i^k + v_i^{k+1} \tag{10}$$

Here, x_i^k is the position and v_i^k is the velocity, while c_1^k and c_2^k are constants expressing acceleration that moves each particle to the $pbest$ and $gbest$ positions. c_1^k allows movement of the particle according to its own experiences, and c_2^k allows the movement of the particle according to the experiences of other particles in the swarm. $rand_1$ and $rand_2$ are uniformly distributed random numbers in the range of [0,1].

Step 6: Did the number of iterations end?

Step 7: Go to Step 2 if the number of iterations did not end.

Step 8: If the iterations ended, calculate the average of the brightness values at the end positions of the particles and select the new value as the iterative threshold value.

According to the steps of the algorithm, the first 500 particles are distributed on random pixels in the image, and these pixel values are assumed as the brightness value of the particles. The objective function used in the PSOA is the same as the objective function used in the FFA. In the proposed algorithm, the movement of particles is carried out towards the particles with low brightness by comparing the brightness of particles according to Eqs. (9) and (10). This algorithm was repeated 50 times, and the brightness average of the positions of particles was chosen as the threshold value. Figure 6 shows the images obtained with the PSOA.

Figure 6. a) Distribution of particles in the image, b) hemorrhage detection by thresholding, c) areas containing hemorrhage in the retina.

As shown in Figure 6, a different threshold value was generated in each image through iterative threshold values generated by the PSOA to detect the areas containing hemorrhage in the retina. The accurate classification rates and time performances of the threshold values obtained by both algorithms were compared.

2.2.4. Classification

In the classification step, DR disease detection was performed by using the feature dataset consisting of the number of hemorrhagic pixels and the number of hemorrhagic regions obtained by the FFA and PSOA-based iterative thresholding as input to the LR-based classifier. Regression analysis, which provides a linear equation between input and output, is among the most basic and computationally inexpensive classification methods. The univariate LR equation used in the classification method is given in Eq. (11).

$$\begin{aligned} y &= f(x,w) = w_0 + w_1 x_1 + ... + w_d x_d \\ &= w_0 + x^T w_1 \end{aligned} \tag{11}$$

Here, the most commonly used method to find the value of the w_0 and w_1 terms is the least squares (LMS) method [38]. Eq. (12), which provides error minimization, is used in the calculation of these coefficients.

$$w_i = \frac{1}{n} \sum_{i=1}^{n} \left(y_i - f(x_i, w) \right)^2 \tag{12}$$

After the coefficients of the regression function are determined in Eq. (12), Eq. (11) is applied to the test dataset. The values obtained were compared with the threshold value of 0.5 determined as a result of the experimental studies and the disease diagnosis was performed. The main disadvantage of the LR used as a classifier is that it requires a threshold value in the decision-making step. In order to prevent this, the SVM, which is known as a good classifier method, has also been used in the study. The SVM is a classifier based on statistical learning theory. The purpose of this method is to estimate the most appropriate decision function that can distinguish two classes [39]. With the decision function, the most suitable hyperplane is determined, which can distinguish training data. The equations for the support vectors in the SVM are given in Eq. (13) to be used in a binary classification problem that can be differentiated linearly.

$$\begin{aligned} wx + b = +1, y = +1 \\ wx + b = -1, y = -1 \end{aligned} \tag{13}$$

Here, y is the class label, w is the weight vector, and b is the value of approximation. To increase m, the value of the optimum plane spacing, it is necessary to minimize the value of w as shown in Eq. (14).

$$m = \frac{2}{\sqrt{ww}}, f_{min}(w) = \frac{ww}{2} \tag{14}$$

Based on Eq. (15),

$$\begin{aligned} &y_i(wx_i + b) - 1 \geq 0 \\ &L(w, b, a) = \frac{w^2}{s} - \sum_{i=1}^{k} a_i y_i(wx_i + b) + \sum_{i=1}^{k} a_i, \end{aligned} \tag{15}$$

the equation obtained is solved by Lagrange equations. The decision function of the SVM for a two-class problem is given in Eq. (16) [40].

$$f(x) = sign(\sum_{i=1}^{k} a_i y_i(xx_i) + b) \tag{16}$$

3. Results and discussion

We focused on the detection of hemorrhages, which are a crucial step in DR disease. For this purpose, the total hemorrhagic pixel counts and hemorrhagic region counts were obtained by applying color space selection, brightness-contrast adjustment, adaptive histogram equalization, Gabor transformation, Top-hat transformation, and FFA/PSOA-based iterative thresholding, respectively, in the retinal images, and then those were used as inputs in the LR-based and SVM-based classifiers for the detection of DR disease. In order to prevent the LR-based and SVM-based classifiers from overfitting, the K-fold cross-validation method was applied, which allows testing and validating the available data. This validation method randomly selects data points for the sets of training, test, and validation. In this study, the K value was taken as 5, and the available data were divided into five parts. Three of them were combined to be used as training data, and the other two parts were used as the test data. The above procedure was repeated five times, using two parts selected for the test each time, and five test results were obtained. The average of these values, which is the accurate classification rate, was considered the general measure of success.

3.1. Validity criteria

The following statistical measures are used to see the overall success of the LR-based classifier and the SVM model used in the study.

True positive (TP): The number of correctly classified hemorrhagic individuals.

True negative (TN): The number of correctly classified nonhemorrhagic individuals.

False positive (FP): The number of individuals who were found to have a hemorrhage by mistake, but were not hemorrhagic.

False negative (FN): The number of individuals who were found to have no hemorrhage by mistake, but were hemorrhagic.

Using these criteria, the sensitivity, specificity, and total correct classification (TCC) ratios are calculated using Eqs. (17)–(19) below:

$$Sensitivity = \frac{TP}{TP + FN} \tag{17}$$

$$Specificity = \frac{TN}{TN + FP} \tag{18}$$

$$TCC = \frac{TP + TN}{TP + FP + TN + FN} \tag{19}$$

The sensitivity rate in Eq. (17) is the probability of distinguishing the real patients among the given patient group. The specificity rate in Eq. (18) is the probability of distinguishing the real strong ones from the others. The total correct classification rate in Eq. (19), which is one of the criteria used when a single criterion is desired by combining sensitivity and specificity, is obtained by dividing the rate of patients and healthy individuals in the test by the total correct diagnosis rate. In the case of a higher success rate, the confusion matrix and ROC curve analysis are used to make a general assessment [41]. Tables 2 and 3 show the confusion matrices for the successes of the models obtained by LR-based and SVM-based classifiers that use FFA and PSOA-based iterative thresholding methods.

Table 2. Resulting confusion matrices obtained using FFA-LR and FFA-SVM.

a) FFA-LR

Class	Healthy	Hemorrhage
Healthy	16	4
Hemorrhage	3	17

b) FFA-SVM

Class	Healthy	Hemorrhage
Healthy	17	3
Hemorrhage	3	17

Table 3. Resulting confusion matrices obtained using PSOA-LR and PSOA-SVM.

a) PSOA-LR

Class	Healthy	Hemorrhage
Healthy	18	2
Hemorrhage	1	19

b) PSOA-SVM

Class	Healthy	Hemorrhage
Healthy	19	1
Hemorrhage	0	20

As shown in Table 2 and Table 3, 13 cases were incorrectly classified by FFA iterative thresholding, whereas the PSOA-based iterative thresholding misclassified only 4 cases in total. Although there were 3 false positives with the LR-based classifier that uses PSOA-based iterative thresholding, there was only 1 false positive with the SVM-based classifier. The results represent the highest successes achieved in 4 different models.

Table 4 shows the validity results of the models created by LR and SVM-based classifiers that use inputs from the dataset consisting of total hemorrhagic pixel count and number of hemorrhagic regions obtained by FFA and PSOA-based iterative thresholding in the retinal image.

Table 4. FFA/PSOA-based thresholding methods and sensitivity, specificity, and TCC ratios of LR/SVM models.

Method	LR			SVM		
	Sensitivity	Specificity	TCC	Sensitivity	Specificity	TCC
Thresholding with FFA	0.915	0.865	0.89	0.922	0.873	0.897
Thresholding with PSOA	0.955	0.905	0.93	0.967	0.914	0.941

As shown in Table 4, the model that uses PSOA thresholding and the SVM-based classifier for the detection of hemorrhage in the retinal image seems to be more successful than the other models. Figure 7 shows the ROC curves obtained using the sensitivity and specificity values calculated for these models.

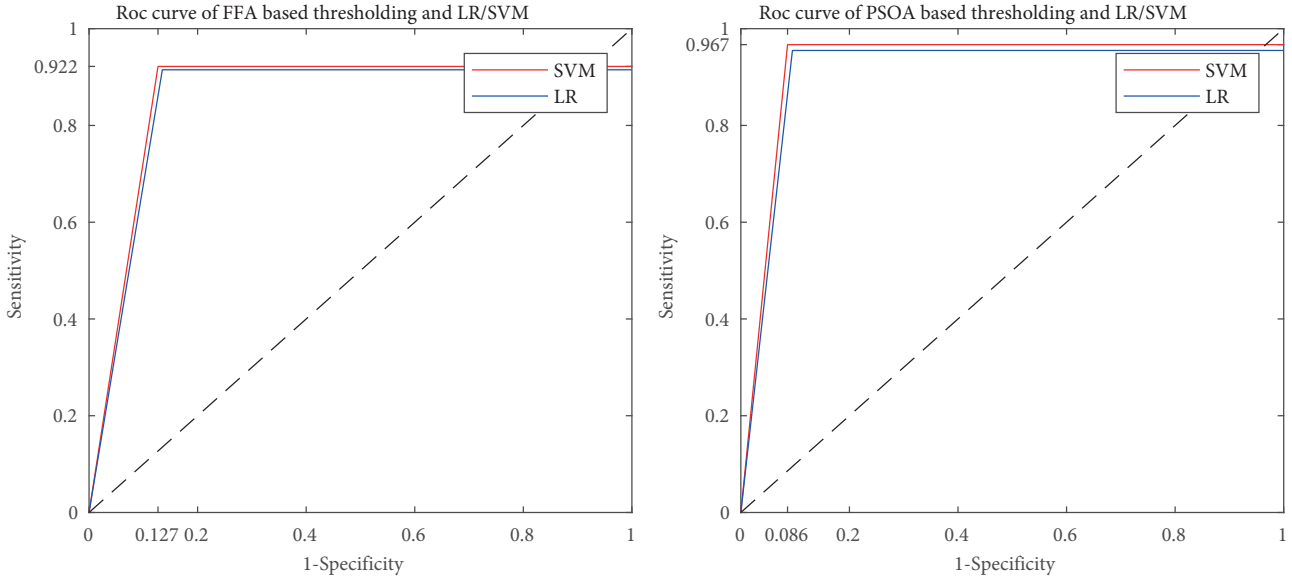

Figure 7. ROC curves of FFA/PSOA-based thresholding LR/SVM classifier.

When the area under the ROC curves in Figure 7 is examined, it is seen that the correct classification rate obtained with PSOA-based thresholding for the detection of hemorrhagic patients is higher than that of the FFA-based thresholding. However, when the thresholds made with PSOA were examined, it was seen that the SVM provided more successful classifier model results than the LR-based classifier. Table 5 shows the number of data, methods used for feature extraction, and success rates reported in the proposed studies and studies in the literature on the detection of hemorrhages.

As shown in Table 5, when the studies for the detection of hemorrhages are examined, it is seen that PSOA-based iterative thresholding and the SVM classifier reached the total correct classification ratio of 94.1%, which is higher than the other studies in the literature. It is thought that this success ratio will increase further with increasing image quality. Another parameter as important as the correct classification rate is the time performance of these two algorithms. The execution times of the thresholding algorithms with the FFA and PSOA are given in Table 6.

Table 5. Techniques and success rates used in studies related to the detection of hemorrhage.

Authors	Year	Data number	Method	Sens	Spec	TCC (%)
Raja and Vasuki	2015	89	Gabor, Bayes	-	-	93.76
Romero et al.	2015	89	Bottom-hat, radon, PCA	88.06	97.47	92.19
Kaur et al.	2016	50	Morphological operations, SVM	90.42	92.53	89.23
van Grinsven et al.	2016	1200	Convolutional neural networks (CNNs)	93.1	91.5	-
Zhou et al.	2016	130	Statistical features, SVM	95	82	-
Srivastava et al.	2017	143	Multiple kernel learning	-	-	91.9
Mumtaz et al.	2018	89	Gamma correction, global thresholding	84	87	89
Lam et al.	2018	243	CNNs	-	-	86
Proposed method-1	2018	100	Gabor, Top-hat, threshold with FFA, regression	91.5	86.5	89
Proposed method-2	2018	100	Gabor, Top-hat, threshold with FFA, SVM	92.2	87.3	89.7
Proposed method-3	2018	100	Gabor, Top-hat, threshold with PSOA, regression	95.5	90.5	93
Proposed method-4	2018	100	Gabor, Top-hat, threshold with PSOA, SVM	96.7	91.4	94.1

Table 6. Time performance of the FFA/PSOA thresholding methods and system.

Method	Time performance of iterative thresholding (s)	Running time performance of system (s)
Thresholding with FFA, SVM	6.28	6.76
Thresholding with PSOA, SVM	0.71	1.19

As shown in Table 6, when the time performance of the thresholding methods is compared, PSOA-based thresholding seems to run about 9 times faster than the other thresholding method. In the FFA-based thresholding, only the brightness values of the two fireflies are taken into account when the fireflies are displaced; on the other hand, the brightness values of all particles are taken into account in the PSOA-based thresholding. This makes the displacement function of particles used in PSOA more effective. In addition, when the running time performance of the overall system is examined, it is seen that the PSOA-based thresholding is advantageous compared to the other method. For this reason, iterative thresholding with PSOA has been proposed as the thresholding method in the study. Detection of hemorrhagic retinal images was performed by classifying the feature set, extracted by the thresholding algorithm, using the SVM.

In order to evaluate the success of the proposed methods in a different image database, we also reimplemented our approach for the ImageRet database, which is widely used and publicly available for DR diagnosis and consists of 89 retina images. The experimental results illustrated that the sensitivity, specificity, and TCC ratios of the PSOA and SVM methods for the GopRetina database were 96.7%, 91.4%, and 94.1%, respectively, whereas these success ratios of the same methods for the ImageRet database were 95%, 91.1%, and 93.4%, respectively. As a conclusion, our approaches reached high correct classification ratios for both the GopRetina and ImageRet databases.

4. Conclusion

In this paper, a diagnostic decision support system was proposed for detecting hemorrhages, which is one of the signs of diabetic retinopathy diseases. This system consists of the enhancement of the image using basic preprocessing methods, the segmentation of vessels with the help of Gabor and Top-hat transformation for the removal of the vessels from the image, the determination of the number of regions with hemorrhages and pixel counts in these regions using FFA/PSOA-based iterative thresholding, and the detection of hemorrhages with the help of the SVM/LR-based classifier. The experimental studies showed that the SVM classifier reached higher rates of accurate classification. In future works, the proposed system will be based on increasing the specificity and sensitivity values. This success rate proves that it can be used as a medical decision support system for detecting hemorrhage, which is one of the important stages of diabetic retinopathy disease.

References

[1] Klein R, Klein BE, Moss SE, Davis MD, DeMets DL. The Wisconsin epidemiologic study of diabetic retinopathy. III. Prevalence and risk of diabetic retinopathy when age at diagnosis is 30 or more years. Arch Opht 1984; 102: 527-532.

[2] Yau JW, Rogers SL, Kawasaki R. Global prevalence and major risk factors of diabetic retinopathy. Diab Care 2012; 35: 556-564.

[3] Hiller R, Sperduto RD, Podgor MJ, Ferris FL, Wilson PW. Diabetic retinopathy and cardiovascular disease in type II diabetics. The Framingham Heart Study and the Framingham Eye Study. Am J Epid 1988; 128: 402-409.

[4] Klein R, Klein BE, Moss SE, Cruickshanks KJ. Association of ocular disease and mortality in a diabetic population. Arch Opht 1999; 117: 1487-1495.

[5] Gönül Ş, Kadıoğlu E. Retina sinir lifi tabakası ve diyabet. Tıp Araşt Derg 2013; 11: 87-93 (in Turkish).

[6] Spencer T, Olson JA, McHardy KC, Sharp PF, Forrester JV. An image processing strategy for the segmentation and quantification of microaneurysms in fluorescein angiograms of the ocular fundus. Comput Biomed Res 1996; 29: 284-302.

[7] Frame AJ, Undrill PE, Cree MJ, Olson JA, McHardy KC, Sharp PF, Forrester JV. A comparison of computer based classification methods applied to the detection of microaneurysms in ophthalmic fluorescein angiograms. Comput Biolgy Med 1998; 28: 225-238.

[8] Streeter L, Cree MJ. Microaneurysm detection in colour fundus images. Img Vsn Comp 2003; 280-284.

[9] Kande GB, Savithri TS, Subbaiah PV. Automatic detection of microaneurysms and hemorrhages in digital fundus images. J Digit Imaging 2010; 23: 430-437.

[10] Li Q, You J, Zhang D. Vessel segmentation and width estimation in retinal images using multiscale production of matched filter responses. Exp Syst Appl 2012; 39: 7600-7610.

[11] Zhang X, Fan G. Retinal spot lesion detection using adaptive multiscale morphological processing. Lect Notes Comp Sci 2006; 4292: 490-501.

[12] Shivaram JM, Patil R, Anarind HS. Automated detection and quantification of hemorrhages in diabetic retinopathy images using image arithmetic and morphological methods. Int J Recent Trends Eng 2009; 2: 174-176.

[13] Walter T, Massin P, Erginay A, Ordonez R, Jeulin C, Klein JC. Automatic detection of microaneurysms in color fundus images. Med Img Anal 2007; 11: 555-566.

[14] Kleawsirikul N, Gulati S, Uyyanonvara B. Automated retinal hemorrhage detection using morphological top hat and rule-based classification. In: 3rd International Conference on Intelligent Computing Systems; 2013. pp. 39-43.

[15] Rosas-Romero R, Martínez-Carballido J, Hernández-Capistrán J, Uribe LJ. A method to assist in the diagnosis of early diabetic retinopathy: image processing applied to detection of microaneurysms in fundus images. Comput Med Img Graph 2015; 44: 41-53.

[16] Quellec G, Lamard M, Josselin PM, Cazuguel G, Cochener B, Roux C. Optimal wavelet transform for the detection of microaneurysms in retina photographs. IEEE T Med Imaging 2008; 27: 1230-1241.

[17] Akram MU, Khan SA. Automated detection of dark and bright lesions in retinal images for early detection of diabetic retinopathy. J Med Sys 2012; 36: 3151-3162.

[18] Ramlugun GS, Nagarajan VK, Chakraborty C. Small retinal vessels extraction towards proliferative diabetic retinopathy screening. Exp Syst Appl 2012; 39: 1141-1146.

[19] Akram MU, Khalid S, Khan SA. Identification and classification of microaneurysms for early detection of diabetic retinopathy. Patt Recogn 2013; 1: 107-116.

[20] Akram MU, Khalid S, Tariq A, Khan SA, Azam F. Detection and classification of retinal lesions for grading of diabetic retinopathy. Comput Bio Med 2014; 45: 161-171.

[21] Sopharak A, Uyyanonvara B, Barman S. Simple hybrid method for fine microaneurysm detection from non-dilated diabetic retinopathy retinal images. Comput Med Img Graph 2013; 37: 394-402.

[22] Raja SS, Vasuki S. Screening diabetic retinopathy in developing countries using retinal images. App Med Inf 2015; 36: 13-22.

[23] Gardner GG, Keating D, Williamson TH, Elliott AT. Automatic detection of diabetic retinopathy using an artificial neural network: a screening tool. Brit J Ophthalmol 1996; 80: 940-944.

[24] Zhou L, Li P, Yu Q, Qiao Y, Yang J. Automatic hemorrhage detection in color fundus images based on gradual removal of vascular branches. In: Image Process Conference (ICIP); 2016. pp. 399-403.

[25] van Grinsven MJ, van Ginneken B, Hoyng CB, Theelen T, Sánchez CI. Fast convolutional neural network training using selective data sampling: application to hemorrhage detection in color fundus images. IEEE T Med Img 2016; 35: 1273-1284.

[26] Kaur N, Kaur J, Accharya M, Gupta S. Automated detection of red lesions in the presence of blood vessels in retinal fundus images using morphological operations. In: ICPEICES; 2016. pp. 1-4.

[27] Mumtaz R, Hussain M, Sarwar S, Khan K, Mumtaz S, Mumtaz M. Automatic detection of retinal hemorrhages by exploiting image processing techniques for screening retinal diseases in diabetic patients. Int J Diabetes Dev C 2018; 38: 80-87.

[28] Lam C, Yu C, Huang L, Rubin D. Retinal lesion detection with deep learning using image patches. Invest Opht Vis Sci 2018; 59: 590-596.

[29] Neto LC, Ramalho GL, Neto JFR, Veras RM, Medeiros FN. An unsupervised coarse-to-fine algorithm for blood vessel segmentation in fundus images. Exp Syst Appl 2017; 78: 182-192.

[30] Srivastava R, Duan L, Wong DW, Liu J, Wong TY. Detecting retinal microaneurysms and hemorrhages with robustness to the presence of blood vessels. Comput Bio Med 2017; 138: 83-91.

[31] Pal R, Pal K. A review on image segmentation techniques. Pattern Recogn 1993; 26: 1277-1294.

[32] Gonzales RC, Woods RE. Digitial Image Processing. Upper Saddle River, NJ, USA: Prentice Hall, 2002.

[33] Yoon H, Han Y, Hahn H. Image contrast enhancement based sub-histogram equalization technique without over-equalization noise. International Journal of Computational Science and Engineering 2009; 3: 1-10.

[34] Petkov N, Wieling BM. Gabor filter augmented with surround inhibition for improved contour detection by texture suppression. Groningen, the Netherlands: Institute for Mathematics and Computing Science, 2004.

[35] Yavuz Z, Köse C. Retinal blood vessel segmentation using Gabor filter and top-hat transform. In: Signal Processing and Communications Conference (SIU); 2011. pp. 546-549.

[36] Yang XS. Nature-inspired Metaheuristic Algorithms. New York, NY, USA: Luniver Press, 2008.

[37] Eberhart R, Kennedy J. A new optimizer using particle swarm theory. In: Micro Machine and Human Science MHS'95; 1995. pp. 39-43.

[38] Chapra SC, Canale RP. Yazılım ve Programlama Uygulamalarıyla Mühendisler İçin Sayısal Yöntemler. Ankara, Turkey: Literatür Yayıncılık, 2003 (in Turkish).

[39] Vapnik V. The support vector method of function estimation. In: In: Suykens JAK, Vandewalle J, editors. Nonlinear Modeling. New York, NY, USA: Springer, 1998. pp. 55-85.

[40] Osuna EE, Freund R, Girosi F. Support Vector Machines: Training and Applications. Cambridge, MA, USA: MIT, 1997.

[41] Bishop CM. Neural Networks for Pattern Recognition. Oxford, UK: Oxford University Press, 1995.